4th International Conference on Computational and Mathematical Biomedical Engineering - CMBE2015
29 June-1 July 2015, France
P. Nithiarasu and E. Budyn (Eds.)

HYBRID CELL CENTRED/VERTEX MODEL FOR CELLULAR MONOLAYERS

Payman Mosaffa[1], Nina Asadipour[1], Daniel Millán[1], Antonio Rodríguez-Ferran[1], and Jose J. Muñoz[1]

[1]Laborati de Càlcul Numèric (LaCàN), Dept. Applied Mathematics III, Universitat Polit'ècnica de Catalunya, Urgell 187, 08036, Barcelona , Spain {payman.mosaffa, nina.asadi, daniel.millan, antonio.rodriguez-ferran, j.munoz}@upc.edu

SUMMARY

Macroscopic deformations in embryonic soft tissues are due to the intra-cellular remodelling and cell intercalation. We here present a computational approach that can handle the two types of deformations, and also take into account the active cell response. The model resorts to cell centred techniques, where particles represent cell nuclei, and to vertex models, where the vertices represent cell boundaries. This hybrid approach allows to consider separately intra-cellular and inter-cellular forces, and at the same time impose cell incompressibility. The model is applied to simulate the active stretching of epithelium.

Key words: *cell centred model, vertex model, remodelling, cell intercalation, epithelium, monolayer*

1 INTRODUCTION

The observed deformations of embryonic multicellular tissues is governed by multiple proteins that mediate the activity of the cytoskeleton [4] and at also by adhesive proteins that control inter-cellular contact (cadherins, lime, catenins,...) [1]. The macroscopic shape changes are the result of the contributions of the two types of forces, which together strongly influence cell polarisation and intercalation [9]. When simulating characteristic morphological processes such as germ band extension [4], it is crucial to properly handle the connectivity changes that take place during cell reorganisation, and at the same time capture the polymeric material of the cell.

From the computational standpoint, cell-centred models focus on the force balance between cell nuclei [5], while in vertex models mechanical equilibrium is applied at the cell-cell junctions [3, 8]. In order to capture the two types of approaches, we here propose a hybrid model that combines mechanical equilibrium at cell centres, but also includes mechanical constraints at the associated vertex points in order to simulate cell incompressibility.

2 METHODOLOGY

2.1 Tissue definition

We will consider cellular tissues with a constant number of cells N, and located on a sufficiently regular manifold, not necessarily flat. The tissue kinematics is defined at each discrete time instants t_n by the cell-cell connectivity, here denoted by $\boldsymbol{T}_n$, and the positions of the cell centres $\boldsymbol{X}_n = [\boldsymbol{x}_n^1, \dots, \boldsymbol{x}_n^N]$, with $\boldsymbol{x}_n^i$ the position of cell i at time t_n. We denote by $\boldsymbol{C}_n = \{\boldsymbol{X}_n, \boldsymbol{T}_n\}$ the configuration of the tissue at time t_n which fully describes its kinematics.

At each time increment, the new configuration $\boldsymbol{C}_{n+1}$ is searched from the previous comfiguration $\boldsymbol{C}_n$ by solving the following two step process [6]:

S1. Find the mechanically equilibrated positions $\boldsymbol{X}_{n+1}$ maintaining the connectivity $\boldsymbol{T}_n$ constant.

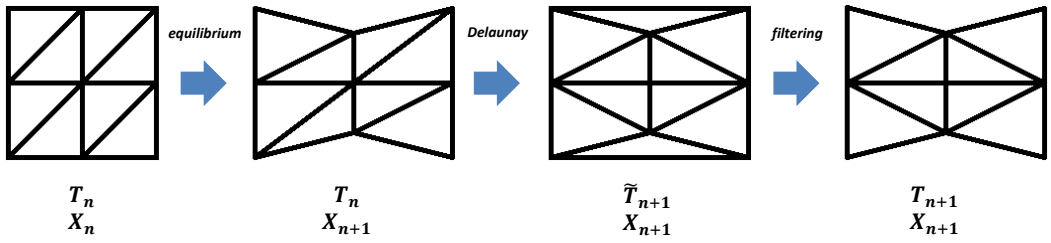

Figure 1: Computational process for retrieving positions and connectivity $\boldsymbol{X}_{n+1}$ and $\boldsymbol{C}_{n+1}$ from the same quantities at time t_n.

S2 Find the new connectivity $\boldsymbol{T}_{n+1}$ maintaining the centre positions $\boldsymbol{X}_{n+1}$.

The new set $\{\boldsymbol{X}_{n+1}, \boldsymbol{T}_{n+1}\}$ defines the new configuration $\boldsymbol{C}_{n+1}$. Step S1 is here resolved by solving equilibrium of all the forces at each cell-centre (particles). The new connectivities are instead found resorting to Delaunay triangulation, which is here adapted to obtain connectivity patterns that are convex and not necessarily flat. Figure 1 illustrates the two step process, where the process S2 comprises the Delaunay and the filtering stages. The next two sections detail the steps S1-S2.

2.2 Mechanical equilibrium

The cell-cell connectivity defined by $\boldsymbol{T}_n$ includes information on the set of N_i particles $I_i = \{i_1, \dots, i_{N_i}\}$ connected to each particle i. Each pair of connected particles $\{i, j\}$ are joined with a bar element that represents the forces between the two cells. This force is derived here from an elastic potential,

$$V^{ij} = \frac{L}{2} k \left(\varepsilon^{ij}\right)^2 \tag{1}$$

where $\varepsilon^{ij} = \frac{l^{ij} - L^{ij}}{L^{ij}}$ is the scalar elastic strain, and $l^{ij} = ||\boldsymbol{x}^i - \boldsymbol{x}^j||$ and L are the *current* and *reference lengths*. We note that the latter is not necessarily equal to the initial length $L_0^{ij} = ||\boldsymbol{x}_0^i - \boldsymbol{x}_0^j||$. The traction force at particle i is then given by (no summation on i):

$$\boldsymbol{t}^{ij} = \frac{\partial V^{ij}}{\partial \boldsymbol{x}^i}$$

Mechanical equilibrium is then computed by solving the following set of equations:

$$\sum_{j \in I_i}^{N_i} \boldsymbol{t}^{ij} = 0, \; i = 1, \dots, N$$

which is equivalent to minimising the total elastic energy of the system $V = \sum_i^N \sum_{j \in I_i}^{N_i} V^{ij}$. The methodology is equivalent to the one employed in standard particle systems [2]. The main particularity is the use of the potential in (1), which includes the reference length L^{ij}. When this length is equal to L_0^{ij}, the elements are equivalent to standard linear elastic bars (although the resulting equations are non-linear due to the change of direction of $\boldsymbol{t}^{ij}$). If instead L^{ij} is allowed to vary, this quantity is understood as an additional internal variable. In this case, it is necessary to

(i) define its evolution law, and

(ii) set a strategy to update the reference length for newly connected particles.

2.2.1 Evolution law of active length L

We will assume that the cells adapt their resting length according to their strain state, so that they tend to relax. Such behaviour can be described according to the following evolution law for [7],

$$\dot{L}^{ij} = \gamma$$

where γ is the *remodelling rate*, a material parameter that measures the ability of the polymeric cytoskeleton to adapt to the imposed strain. It has been shown that the resulting response is equivalent to a Maxwell-like model.

2.2.2 Update of active length L

In order to define a resting length for any arbitrary direction, we define at each particle i the *active length tensor* $\mathbf{L}^i$, which contains information on the distribution of the resting length around point $\boldsymbol{x}^i$, in a similar manner to the strain tensor in continuum mechanics. The active length along direction $\boldsymbol{n}$ is computed as

$$L_n = \boldsymbol{n} \cdot \mathbf{L} \cdot \boldsymbol{n}$$

The computation of tensor $\mathbf{L}$ is achieved by minimising the error of the previous expression with respect the existing directions n^{ij} around a particle i (see [6] for further details):

$$L^i = \text{argmin}_{\mathbf{L}} \sum_{j \in I_i} ||L^{ij} - \boldsymbol{n}^{ij} \cdot \mathbf{L} \cdot \boldsymbol{n}^{ij}||^2$$

2.3 Cell-cell connectivity: Delaunay triangulation and Voronoi tessellation

Once the set of new positions $\boldsymbol{X}_{n+1}$ has been obtained, the connectivity between the particles is obtained resorting to a Delaunay algorithm on the whole set of particles. Due to the new positions, the new connectivity $\boldsymbol{T}_{n+1}$ may differ from the previous connectivity $\boldsymbol{T}_n$. Furthermore, due to the fact that standard Delaunay triangulations yield a convex polytope, and that the set of particles form a curved manifold, the algorithm is modified by,

(a) excluding triangles (or tetrahedra in 3D) that have a very high aspect ratio, and

(b) mapping the set of particles on a flat surface, and using the resulting two-dimensional triangulation on the curved manifold.

The process in (b) is illustrated in Figure 2, where the mapping of the particles on a curved manifold to the flat surface is represented by $\boldsymbol{\varphi}(\boldsymbol{X})$.

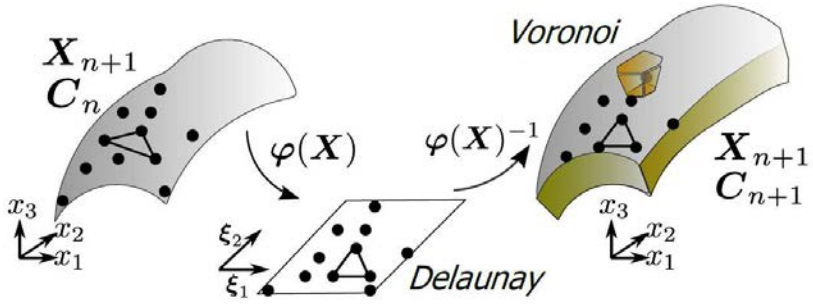

Figure 2: Schematic of the mapping employed for applying Delaunay triangulation on curved monolayers.

In addition, since the particles represent cell centres (nuclei), we will use a Voronoi tessellation of the Delaunay network in order to represent the cells. Due to the fact that standard Voronoi tessellations give unbounded domains with vertices located at infinity, we have added some "phantom" particles at the boundary of the tissue. Furthermore, when cells are on a curved manifold (monolayer or epithelium), we also added "phantom" offset particles above and below the manifold in order to retrieve the bounded domain of the cells. Such Voronoi vertices can be interpolated on the domain of the particles, and used to impose mechanical constraints or incompressibility of the individual cells.

3 RESULTS AND CONCLUSIONS

We have applied the previous model to flat and curved stretched monolayers. Figure 3b shows the deformed shape of a cylindrical tissue subjected to imposed displacements at one of its ends, and undergoing connectivity changes with a variable resting length. We have quantified the non-linear response due to the distinct contributions of the cell reorganisation and the resting length changes. Both have very different origin, and can be modulated independently in our model. Although no cell activity has been implemented, we expect to do so in order to better mimic the in-plane reorganisation of embryonic tissues [9].

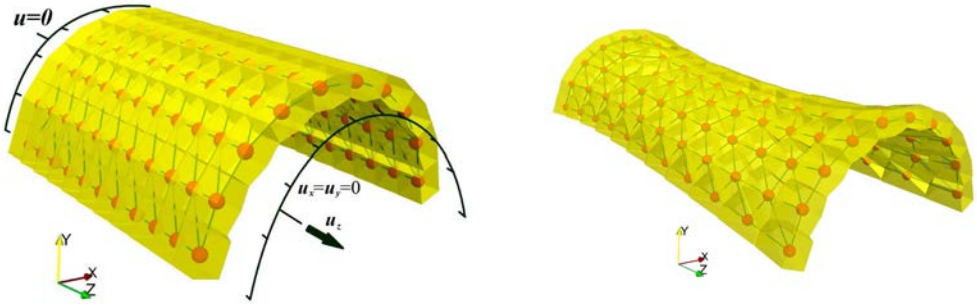

(a) (b)

Figure 3: (a) Initial and (b) deformed shape for the curved monolayer test.

REFERENCES

[1] A Brugués, E Anon, V Conte, JH Veldhuis, M Gupta, J Collombelli, J J Muñoz, GW Brodland, B Ladoux, and X Trepat. Forces driving epithelial wound healing. *Nature Phys.*, 10:683–690, 2014.

[2] M Griebel and S Knapek nad GZumbusch. *Numerical Simulation in Molecular Dynamics. Numerics, Algorithms, Parallelization, Applications*, volume 5 of *Texts in Computational Science and Engineering*. Wiley-Interscience, 2007.

[3] H Honda, M Tanemura, and T Nagai. A three- dimensional vertex dynamics cell model of space-filling polyhedra simulating cell behavior in a cell aggregate. *J. Theor. Biol.*, 226:439–453, 2004.

[4] T Lecuit and P F Lenne. Cell surface mechanics and the control of cell shape, tissue patterns and morphogenesis. *Nature Reviews*, 8:633–644, 2007.

[5] GR Mirams, C J Arthurs, M O Bernabeu, R Bordas, J Cooper, A Corrias, Y Davit, S J Dunn, A G Fletcher, D G Harvey, M E Marsh, J M Osborne, P Pathmanathan, J Pitt-Francis, J Southern, N Zemzemi, and D J Gavaghan. Chaste: An open source c++ library for computational physiology and biology. *PLOS Comp. Biol.*, 9(3):e1002970, 2013.

[6] P Mosaffa, N Asadipour, D Millán, A Rodríguez-Ferran, and J J Muñoz. Cell-centred model for the simulation of curved cellular monolayers. *Comp. Part. Mech.*, 2015. Submitted.

[7] J J Muñoz and S Albo. Physiology-based model of cell viscoelasticity. *Phys. Rev. E*, 88(1):012708, 2013.

[8] S Okuda, Y Inoue, M Eiraku, Y Sasai, and T Adachi. Modeling cell proliferation for simulating three-dimensional tissue morphogenesis based on a reversible network reconnection framework. *Biomech. Model. Mechanobiol.*, 12:987–996, 2013.

[9] M Rauzi, P F Lenne, and T Lecuit. Planar polarized actomyosin contractile flows control epithelial junction remodelling. *Nature*, 468:1110–1114, 2010.